crystals

MDPI

Communication

All-Inkjet Printed Organic Thin-Film Transistors with and without Photo-Sensitivity to Visible Lights

Chen Jiang [1,2]

[1] Department of Engineering, University of Cambridge, 9 JJ Thomson Avenue, Cambridge CB3 0FA, UK; cj360@cam.ac.uk

[2] Department of Clinical Neurosciences, University of Cambridge, Clifford Allbutt Building, Cambridge Biomedical Campus, Cambridge CB2 0AH, UK

Received: 20 July 2020; Accepted: 19 August 2020; Published: 20 August 2020

Abstract: Printable organic thin-film transistors have enabled flexible low-cost electronics, which has the potential for a lot of emerging electronic applications. Despite the excellent dark performance of advanced all-inkjet printed organic thin-film transistors, their photoresponse is less explored and needs to be investigated, especially photoresponse to visible lights that human beings can see and are most familiar with. Importantly, for electronics integration, both devices with and without photo-sensitivity to visible light are important, for photo-detecting and signal processing, respectively. In this study, two organic semiconductor materials are used in all-inkjet printed organic thin-film transistors, namely 2,7-dioctyl[1]benzothieno[3,2-b][1]benzothiophene (C8-BTBT), 6,13-bis (triisopropylsilylethynyl) pentacene (TIPS-pentacene). By characterizing devices under optical exposure with wavelengths from 400 to 800 nm, photocurrents and threshold voltage shifts of the devices are extracted. The fabricated C8-BTBT organic thin-film transistors do not exhibit noticeable photo-sensitivity to visible light, whereas the TIPS-pentacene devices demonstrate significant photoresponse to visible lights, with photocurrents in nano- to micro-ampere levels and threshold voltage shifts of hundreds of millivolts to several volts depending on the photon energy of lights under the same intensity. The TIPS-pentacene devices demonstrated reproducible characteristics before and after light exposure. In addition, the responsivity and sensitivity of the devices were characterized with a decent responsivity of 55.9 mA/W. The photoresponse mechanisms are explained with ultraviolet–visible (UV–vis) adsorption spectroscopy measurements and extracted optical bandgaps of the two semiconductors. This study shows both printed organic transistors with and without photo-sensitivity can be fabricated with the same device structure and fabrication process at low cost, which opens the new possibility of using printed organic thin-film transistors for integrated optoelectronic applications.

Keywords: organic thin-film transistors; inkjet printing; photo-sensitivity; visible lights

1. Introduction

Organic thin-film transistors (OTFTs) have attracted considerable attention in emerging electronics, such as flexible electronics and wearable electronics, due to their features of intrinsic bendability and low-cost printability [1,2]. In the past decades, OTFTs have been applied to various applications, including biosensors [3–5], wearable amplifiers [6,7], and flexible optoelectronic systems [8–10]. However, printed OTFTs typically demonstrate a modest performance, such as with low device mobilities and large operating voltages, which had been bottlenecks for the development of printed OTFTs [11–13]. Recently, a report of all-inkjet printed OTFTs showing a steep subthreshold slope to the thermionic limit has opened up new possibilities of printed electronics for real-world applications [6].

Among various semiconductor applications, optoelectronics is one of the most important branches. There have been plentiful reports on OTFTs used as photodetectors and phototransistors [8], but only sporadic demonstrations by all-printed OTFTs [14,15]. In addition, most of the reports were focused on the response to ultraviolet (UV) lights [8,15,16]. Therefore, it would be interesting to investigate the photo-sensitivity of all-inkjet printed OTFTs, in particular under the visible light exposure that has not been deeply investigated. Furthermore, it is also essential for the real-world applications of photodetectors, printable counterparts that are insensitive to lights to be integrated into a photodetector circuit building block or a system for signal conditioning and processing. Despite examples of using a photo-blocking layer that adds fabrication complexity and cost [17], it is also essential to find some intrinsic methods. Typical organic semiconductors have bandgaps of around 2 eV [6], of which the energy corresponds to a visible light, so they can be used for photo-sensitive OTFTs. To develop photo-insensitive OTFTs, wide-bandgap organic semiconductors (e.g., >3 eV) need to be used. Therefore, to develop all-inkjet printed OTFTs with and without photo-sensitivity to visible light, it is essential to use semiconductors with different bandgaps. However, it still needs to be further explored and validated whether there is a compatible fabrication method for both types of devices without adding fabrication cost and complexity.

In this study, the photoresponse of all-inkjet printed OTFTs to visible lights is investigated. Rather than developing photo-sensitive OTFTs only, an important research question is whether there is a simple OTFT fabrication process used by only a printing technique that can reliably produce both types of OTFTs with and without photo-sensitivity to visible light. To this end, two different organic semiconductors with different bandgaps are designed in the same device structure. The electrical and photo-sensing characteristics of all-inkjet printed OTFTs are measured, and their sensitivity and insensitivity to visible light are investigated.

2. Materials and Methods

2.1. Materials and Ink Formulations

Poly(1,1,2,4,4,5,5,6,7,7-decafluoro-3-oxa-1,6-heptadiene), known as CYTOP (CTL-809M), and its solvent (CT-Solv. 180) were purchased from Asahi Glass, Tokyo, Japan. 2,7-Dioctyl[1]benzothieno [3,2-b][1]benzothiophene (C8-BTBT), 6,13-bis (triisopropylsilylethynyl) pentacene (TIPS-pentacene), polystyrene (PS), polyvinyl cinnamate (PVC), and perfluorobenzenethiol (PFBT) were purchased from Sigma-Aldrich, Gillingham, UK.

The conductive silver (Ag) ink (jet-600C) was supplied by Hisense Electronics, Kunshan, China. The gate dielectric ink was prepared by dissolving PVC in anisole at a concentration of 45 mg/mL. The semiconductor inks were formulated by dissolving C8-BTBT (or TIPS-pentacene) and PS in anisole at a concentration of 10 mg/mL and then mixing the two solutions at a volume-to-volume ratio of 3:1. The addition of PS was to improve the quality of printed semiconductor thin films. For the encapsulation ink, CYTOP was diluted with its solvent at a weight-to-weight ratio of 3:1.

2.2. Device Fabrication

A bottom-gate bottom-contact device structure was used in this study, as shown in Figure 1. A material inkjet printer, DMP-2831(purchased from FUJIFILM Dimatix, Lebanon, New Hampshire, USA), was used for all the fabrication processes, which were conducted in ambient air. All the inks were filled into DMPLCP-11610 cartridges (FUJIFILM Dimatix), of which the nozzles typically jet droplets at the size of around 10 pL. The waveform setting for nozzles was the same as the reported setting in the previous studies [6,18–20].

The Ag ink was printed on a flexible plastic polyethylene naphthalate (PEN) (Teonex®, DuPont, Wilmington, DE, USA) substrate at a drop spacing of 50 µm, followed by annealing at 130 °C for 15 min to form gate electrodes. A single nozzle was used to better control the geometrical precision of printed conductive thin films. Then, the PVC ink was printed at a drop spacing of 10 µm, and 6 consecutive

nozzles were used for jetting at the same time with a cartridge angle of 11.4° (which corresponds to the setting for the drop spacing of 50 µm). Therefore, the actual PVC thin films were printed at a horizontal drop spacing of 10 µm and a vertical drop spacing of 50 µm. The printed PVC film was prebaked at 100 °C for 1 min, exposed to 254 nm UV light for 30 min, and hard-baked at 100 °C for 30 min. The thickness of the printed PVC film was measured to be around 151 nm (of which the unit-area gate capacitance was measured to be 19.9 nF/cm^2). After the formation of the cross-linked PVC gate insulator, the Ag ink was printed again and then annealed at 120 °C for 15 min to form source/drain electrodes of around 100 nm, defining the channel width and length of 1200 µm and 80 µm, respectively. The source/drain electrodes were treated by a 0.1% PFBT-ethanol solution for 3 min and rinsed with ethanol. The semiconductor was printed with 3 consecutive nozzles at a drop spacing of 5 µm and annealed at 60 °C for 30 min. Finally, CYTOP ink was printed to encapsulate the devices and annealed at 60 °C for 30 min.

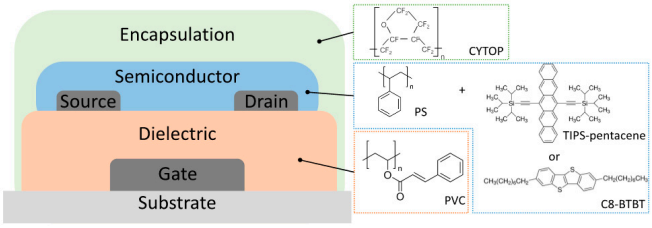

Figure 1. Cross-section of the device structure and materials used.

2.3. Material and Device Characterization

Ultraviolet–visible (UV–vis) spectroscopy measurements of TIPS-pentacene/PS and C8-BTBT/PS films on quartz substrates were made using a UniCam UV-vis spectrometer. The electrical properties of the devices were characterized with a Keithley 4200 Semiconductor Characterization System (Solon, OH, USA). The photoresponse of the devices was measured under LEDs with optical filters centering at wavelengths of 400 nm, 500 nm, 600 nm, 700 nm, and 800 nm. The light intensity for each wavelength was adjusted to 10 mW/cm^2, calibrated by a Thorlabs photodetector DET10A. The LEDs, optical filters, and photodetector were from Thorlabs, Newton, NJ, USA. The illumination area was a circle with a diameter of around 5 mm. The whole area of the channel was irradiated, with the light applied from the top through the CYTOP layer.

2.4. Device Parameters Extraction

The mobility (μ) and threshold voltage (V_T) were calculated by fitting the square root of the drain current (I_D) versus the gate voltage (V_{GS}) using the following equation:

$$I_D = \frac{1}{2}\mu C_i \frac{W}{L}(V_{GS} - V_T)^2, \quad (1)$$

where W is the channel width, L the channel length, and C_i the gate dielectric capacitance per unit area. The subthreshold slope was extracted by fitting the I_D versus V_{GS} in the subthreshold regime using the following equation:

$$I_D = I_{ref} \exp\left(-\frac{V_{GS} - V_{ref}}{SS/\ln(10)}\right), \quad (2)$$

where I_{ref} is the reference current in the subthreshold regime at the reference voltage V_{ref}.

3. Results and Discussion

The electrical transfer and output characteristics of all-inkjet printed C8-BTBT and TIPS-pentacene OTFTs are depicted in Figure 2. Both the devices demonstrated low operating voltages of <3 V and steep subthreshold slopes of <0.2 V/decade compared to typical printed OTFTs, due to the reduced trap

density as reported in the previous studies [6,21]. In comparison, the C8-BTBT devices demonstrated better performance than TIPS-pentacene ones. As shown in Figure 2a, a typical fabricated C8-BTBT OTFT exhibited a field-effect mobility of 0.42 cm^2 V^{-1} s^{-1}, a close-to-zero V_T of 0.11 V, a high on-off ratio of $>10^7$, and a steep subthreshold slope of 64.8 mV/decade. Such a steep subthreshold slope value was close to the thermionic limit of 59.6 mV/decade at room temperature of 300 K. A typical TIPS-pentacene OTFT demonstrated a field-effect mobility of 0.21 cm^2 V^{-1} s^{-1}, a small V_T of −0.21 V, a large on-off ratio of $>10^6$, and a steep subthreshold slope of 142.8 mV/decade. The higher on-off ratio of the C8-BTBT devices was attributed to the reported wideband gap of C8-BTBT [6], so that the off-state current could be lower than the TIPS-pentacene devices. Both the C8-BTBT and TIPS-pentacene OTFTs exhibited negligible hysteresis, as shown in Figure 2a,b.

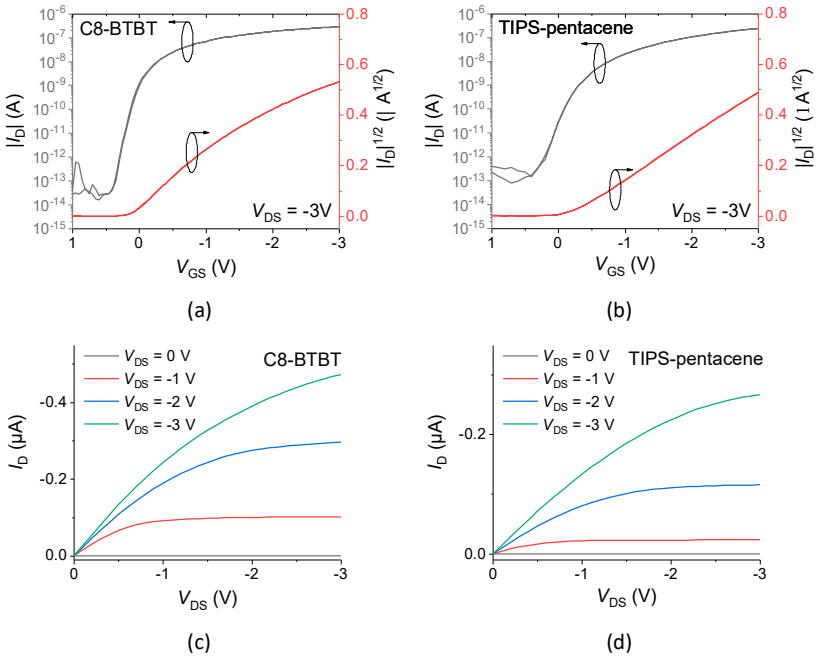

Figure 2. (**a**,**b**) Transfer (I_D–V_{GS}) characteristics and (**c**,**d**) output (I_D–V_{DS}) characteristics of all-inkjet-printed organic thin-film transistors (OTFTs) using (**a**,**c**) 2,7-dioctyl[1]benzothieno[3,2-b][1]benzothiophene (C8-BTBT) and (**b**,**d**) 6,13-bis (triisopropylsilylethynyl) pentacene (TIPS-pentacene) as the semiconductor, respectively.

The most noticeable difference of the device parameter was the steeper subthreshold slope exhibited by the C8-BTBT OTFTs, which can be attributed to the lowered defect density in the C8-BTBT devices. As shown in Figure 3, the printed C8-BTBT thin films formed large flake-like crystals that covered the device channel, whereas the printed TIPS-pentacene thin films had narrow needle-like crystals that consisted of considerable traps at the grain boundaries, which is in line with other reports [21,22]. Despite the overall better performance of C8-BTBT OTFTs, they possessed a large contact resistance when operating in the above-threshold regime (as seen from the non-linearity in the $|I_D|^{1/2}$-V_{GS} plot in Figure 2a, as a result of the presence of a Schottky barrier at the semiconductor-metal contacts. The Schottky barrier was used to achieve a large channel-independent output resistance, which is promising for printed analogue electronics; however, it reduced the charge carrier injection at high current levels in the above-threshold operation, thus limiting its application to displays as active driving transistors. Therefore, for different applications, OTFTs with different materials systems should be designed and selected to maximize their performance.

Although the devices with C8-BTBT and TIPS-pentacene as semiconductors showed minor differences of device performance under dark condition, they behaved notably differently under exposure to visible lights. The C8-BTBT OTFTs demonstrated negligible transfer characteristics changes

under light exposure (400–800 nm), as seen in Figure 4a. In contrast, although TIPS-pentacene OTFTs did not have a response to 800 nm infrared light, they responded actively to visible lights (400–700 nm), as shown in Figure 4b. The negligible response to 800 nm infrared light suggested that the photon energy might be not large enough, given the relation between photon energy (E) and wavelength (λ) as $E = hc/\lambda$, where h is the Planck constant, c is the speed of light in vacuum [23]. The TIPS-pentacene OTFTs started to show photoresponse when the wavelength of exposing light was 700 nm or below, indicating a bandgap of around 1.77 eV.

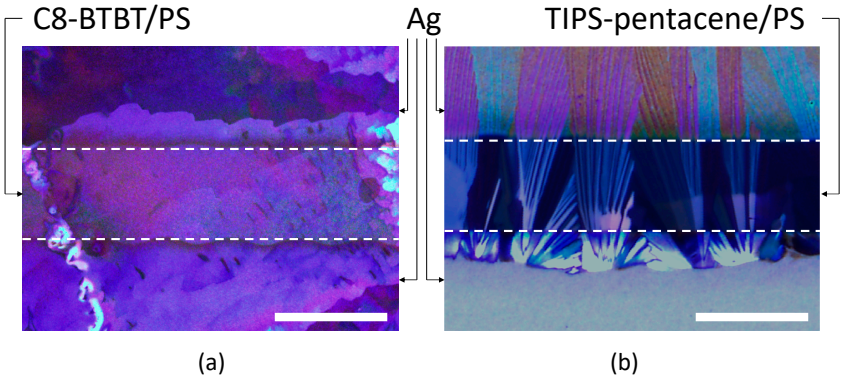

Figure 3. Polarized microscopic photos of printed semiconductor thin films: (**a**) C8-BTBT and (**b**) TIPS-pentacene. Scale bar: 100 μm. Dash lines indicate the boundaries between the source/drain electrodes and channels.

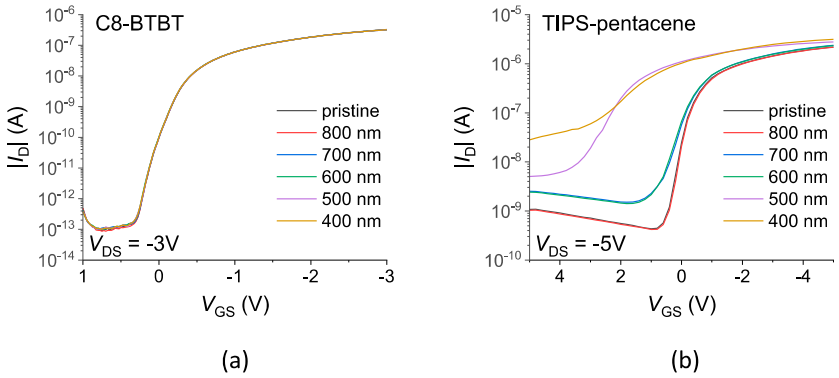

Figure 4. Photoresponse of all-inkjet-printed (**a**) C8-BTBT and (**b**) TIPS-pentacene OTFTs to visible lights with wavelengths of 800 nm, 700 nm, 600 nm, 500 nm, 400 nm.

Photoresponse generally includes two mechanisms: photocurrent and threshold voltage shift [24]. When a semiconductor is exposed to lights (whose photon energy is higher than the bandgap of the semiconductor), excitons are induced. As a result, more free charge carriers are available, which under an electrical field can contribute to a photocurrent. In addition, the excess minority carriers can induce a threshold voltage shift. In this work, the excess charge carriers were electrons, thereby shifting threshold voltage positively. To characterize these effects, photocurrents and threshold voltage shifts were extracted. As shown in Figure 5a, the C8-BTBT OTFTs demonstrated negligible photocurrents under exposure; for TIPS-pentacene, devices demonstrated noticeable photocurrents starting from 700 nm light exposure, and there was a relatively large photocurrent increase from 500 nm to 400 nm light exposure. As for the threshold voltage shifts, the C8-BTBT OTFTs seemed to be free from this effect, as shown in Figure 5b. The TIPS-pentacene demonstrated a gradual increase in threshold voltage shifts with exposure from 800 nm light to 600 nm light and a more significant increase between 600 nm and 500 nm light exposure. The photocurrents were extracted at the V_{GS} of 1 V for both C8-BTBT and TIPS-pentacene OTFTs.

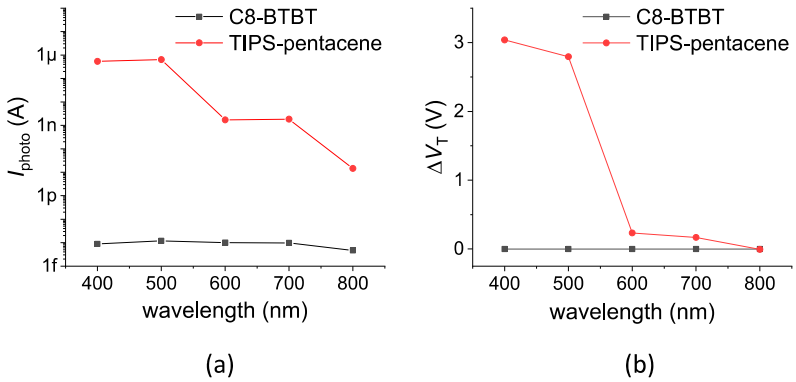

Figure 5. (**a**) Photocurrent (I_{photo}) and (**b**) threshold voltage shift (ΔV_T) of the all-inkjet-printed OTFTs induced by lights with different wavelengths.

As a phototransistor, it is important that the device should have a good reproducibility before and after light illumination. As shown in Figure 6a, the TIPS-pentacene OTFT could recover close to its pristine state, despite a positive shift of around 0.5 V observed in the transfer characteristics curves. Compared to the previously reported printed OTFTs for photodetection [15], the recovery of the fabricated devices in this work seemed better, which could be explained by the reduced trap density in the printed OTFTs. Here, the transfer characteristics shift may be resulted from the slow recovery of the devices after light illumination with a time constant of 10.5 s, as shown in Figure 6b. To improve this slow recovery issue, several studies have reported using gate pulses to instantly switch the phototransistors to the on-state and remove excess charge carriers [16,25]. The responsivity and sensitivity of the TIPS-pentacene OTFT was shown in Figure 6c,d, respectively. For lights with shorter wavelengths, the values for responsivity and sensitivity were higher. In particular, the responsivity was 66.7 mA/W (λ = 500 nm) and 55.9 mA/W (λ = 400 nm), which are comparable to other reported organic phototransistors [8]. The higher responsivity and sensitivity under exposure of lights with shorter wavelengths are attributed to larger photocurrents induced, as depicted in Figure 5a. As seen in Figure 6c,d, the responsivity and sensitivity were very low when the OTFT was exposed to light with the wavelength of 800 nm. For lights with the wavelengths of 600 nm and 700 nm, the responsivity and sensitivity were also not high, as only small changes were seen in the transfer characteristics (Figure 4b). By characterizing the responsivity and sensitivity of the printed TIPS-pentacene OTFTs, one can understand the lights that the devices are most responsive and sensitive to and the shortcomings that need to be improved.

UV–vis spectroscopy was performed to understand the effect of light exposure to the two semiconductors. As shown in Figure 7a, the UV-vis absorption spectrum of C8-BTBT indicated limited light absorbance in the wavelength range from 400 nm to 800 nm, and therefore excitons are not expected to be induced under these lights. In contrast, TIPS-pentacene has a significant increase in light absorbance from 750 nm to 600 nm wavelength lights, as seen in Figure 7b. This could explain the reason that the TIPS-pentacene OTFTs had photoresponse to 700 nm wavelength light, but not 800 nm wavelength light. The absorption spectra for C8-BTBT and TIPS-pentacene were similar to the previous reports by other groups [26,27]. Note that, during the photoresponse characterizations for the fabricated OTFTs, the lights were applied from the top through the CYTOP layer; since CYTOP is a transparent material in the UV–vis–infrared spectra (at wavelengths of 200–2000 nm) [28], the CYTOP encapsulation layer would not affect the absorption of visible lights by the semiconductors and therefore the photoresponse of the OTFTs. With the UV–vis absorption spectra, Tauc plots for the two semiconductors could be obtained and used to find their optical bandgaps. As shown in Figure 7c, the optical bandgap of C8-BTBT was determined to be 3.30 eV, which is in the ultraviolet range. Therefore, the negligible photoresponse of C8-BTBT OTFTs to visible lights can be explained by that the photon energies of visible lights are not high enough to generate an exciton. From the Tauc plot shown in Figure 7d, TIPS-pentacene has two optical bandgaps of 2.58 eV and 1.63 eV, which are

corresponding to cutoff wavelengths of 481 nm and 761 nm. The larger optical bandgap (E_{g1}) is more likely to be related to carrier generation by band-to-band transitions, whereas the smaller optical bandgap (E_{g2}) is related to carrier generation by transitions involving forbidden-gap energy levels, due to the presence of sub-gap trap states of printed TIPS-pentacene thin films [23]. These results suggest different semiconductor materials with smaller bandgaps need to be used to enhance the responsivity and sensitivity of the printed OTFTs to lights with longer wavelengths.

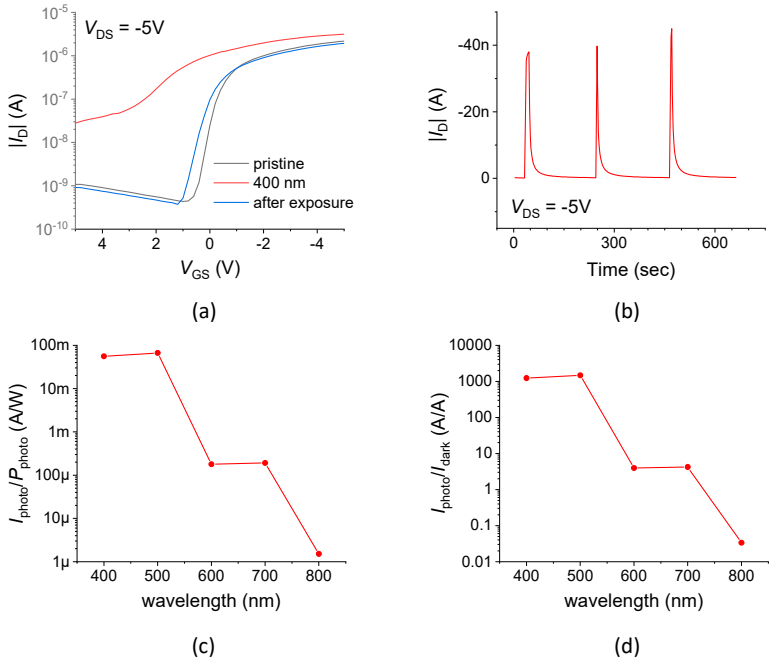

Figure 6. (**a**) The reproducibility of a TIPS-pentacene OTFT before, under, and after exposure to 400 nm light. (**b**) The transient measurement of I_D with light switched on and off. (**c**,**d**) The (**c**) responsivity and (**d**) sensitivity of a TIPS-pentacene OTFT as a function of wavelength.

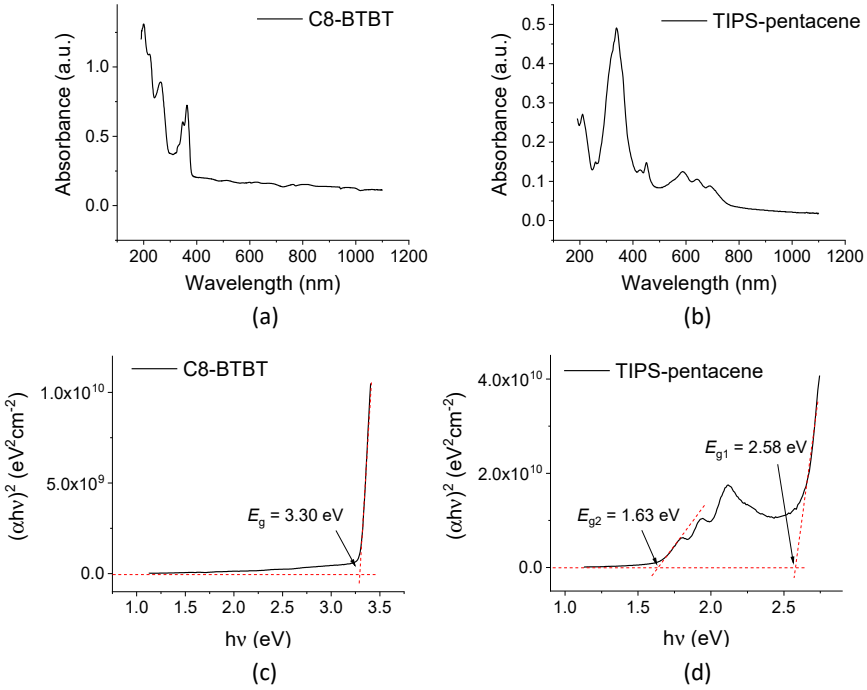

Figure 7. Ultraviolet–visible (UV–vis) absorption spectra of (**a**) C8-BTBT and (**b**) TIPS-pentacene. Tauc plots of (**c**) C8-BTBT and (**d**) TIPS-pentacene.

The mechanism of carrier generation under visible lights is depicted in Figure 8. For C8-BTBT, since the photo energies of visible lights are lower than its optical bandgap, there are no carriers generated by visible light exposure. For TIPS-pentacene, the carriers generated under visible lights include band-to-band transitions and trap-assisted transitions: when the photon energy of exposing light is higher than E_{g2} but lower than E_{g1}, the photocurrent was dominated by carriers generated by trap-assisted transitions; when the photon energy of exposing light is higher than E_{g1}, the photocurrent was dominated by carriers generated by band-to-band transitions, as shown in Figure 8b.

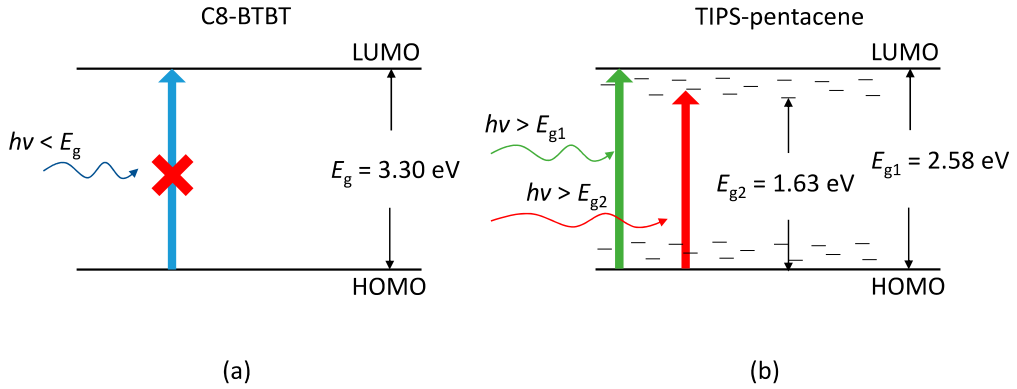

Figure 8. (**a**) Mechanism of no carriers generated in C8-BTBT under visible light exposure. (**b**) Mechanisms of photo-carriers generated in TIPS-pentacene due to band-to-band transitions and trap-assisted transitions under visible light exposure. HOMO: highest occupied molecular orbital. LUMO: lowest unoccupied molecular orbital.

4. Conclusions

This study demonstrated all-inkjet printed OTFTs with and without sensitivity to visible lights. The fabrication of both OTFTs was based on the same method and device structure, while the only difference was the semiconductor materials used. C8-BTBT, the semiconductor material used in photo-insensitive OTFTs, was characterized to have a large optical bandgap of 3.3 eV, so it does not have visible light absorption; TIPS-pentacene, the semiconductor material used in photo-sensitive OTFTs, was characterized to have one of the optical bandgaps in which the photon energy is close to the boundary between visible and infrared lights. In addition, the TIPS-pentacene OTFTs demonstrated a decent photo responsivity of 55.9 mA/W to 400-nm light that is comparable to its vacuum-processed counterparts. This work confirms the possibility to simply integrate the two device technologies into one substrate by one fabrication route. This work would also trigger further study into how to combine photo-sensitive OTFTs as photodetectors and photo-insensitive OTFTs for signal conditioning to build a printable photodetector circuitry or system. In addition, evaluating and improving the photo responsivity and sensitivity of all-inkjet printed organic phototransistors would be another important work for future study.

Funding: This research was funded by the Wellcome Trust under Junior Interdisciplinary Fellowship (204845/Z/16/Z) and the IEEE Electron Devices Society PhD Student Fellowship.

Conflicts of Interest: The author declares no conflict of interest.

References

1. Guo, X.; Xu, Y.; Ogier, S.; Ng, T.N.; Caironi, M.; Perinot, A.; Li, L.; Zhao, J.; Tang, W.; Sporea, R.A.; et al. Current Status and Opportunities of Organic Thin-Film Transistor Technologies. *IEEE Trans. Electron. Devices* **2017**, *64*, 1906–1921. [CrossRef]
2. Jiang, C.; Xiang, C.; Nathan, A. Flexible ultralow power sensor interfaces for e-skin. *Proc. IEEE* **2019**, *107*, 2084–2105. [CrossRef]

3. Lin, P.; Yan, F. Organic thin-film transistors for chemical and biological sensing. *Adv. Mater.* **2012**, *24*, 34–51. [CrossRef] [PubMed]
4. Someya, T.; Bao, Z.; Malliaras, G.G. The rise of plastic bioelectronics. *Nature* **2016**, *540*, 379–385. [CrossRef]
5. Rivnay, J.; Owens, R.M.; Malliaras, G.G. The rise of organic bioelectronics. *Chem. Mater.* **2014**, *26*, 679–685. [CrossRef]
6. Jiang, C.; Choi, H.W.; Cheng, X.; Ma, H.; Hasko, D.; Nathan, A. Printed subthreshold organic transistors operating at high gain and ultralow power. *Science* **2019**, *363*, 719–723. [CrossRef]
7. Wang, S.; Xu, J.; Wang, W.; Wang, G.J.N.; Rastak, R.; Molina-Lopez, F.; Chung, J.W.; Niu, S.; Feig, V.R.; Lopez, J.; et al. Skin electronics from scalable fabrication of an intrinsically stretchable transistor array. *Nature* **2018**, *555*, 83–88. [CrossRef]
8. Baeg, K.J.; Binda, M.; Natali, D.; Caironi, M.; Noh, Y.Y. Organic light detectors: Photodiodes and phototransistors. *Adv. Mater.* **2013**, *25*, 4267–4295. [CrossRef]
9. Street, R.A.; Ng, T.N.; Schwartz, D.E.; Whiting, G.L.; Lu, J.P.; Bringans, R.D.; Veres, J. From printed transistors to printed smart systems. *Proc. IEEE* **2015**, *103*, 607–618. [CrossRef]
10. Yagi, I.; Hirai, N.; Miyamoto, Y.; Noda, M.; Imaoka, A.; Yoneya, N.; Nomoto, K.; Kasahara, J.; Yumoto, A.; Urabe, T. A flexible full-color AMOLED display driven by OTFTs. *J. Soc. Inf. Disp.* **2008**, *16*, 15. [CrossRef]
11. Chung, S.; Kim, S.O.; Kwon, S.K.; Lee, C.; Hong, Y. All-inkjet-printed organic thin-film transistor inverter on flexible plastic substrate. *IEEE Electron. Device Lett.* **2011**, *32*, 1134–1136. [CrossRef]
12. Chang, J.; Zhang, X.; Ge, T.; Zhou, J. Fully printed electronics on flexible substrates: High gain amplifiers and DAC. *Org. Electron.* **2014**, *15*, 701–710. [CrossRef]
13. Sowade, E.; Ramon, E.; Mitra, K.Y.; Martínez-Domingo, C.; Pedró, M.; Pallarès, J.; Loffredo, F.; Villani, F.; Gomes, H.L.; Terés, L.; et al. All-inkjet-printed thin-film transistors: Manufacturing process reliability by root cause analysis. *Sci. Rep.* **2016**, *6*, 33490. [CrossRef] [PubMed]
14. Kim, M.; Ha, H.J.; Yun, H.J.; You, I.K.; Baeg, K.J.; Kim, Y.H.; Ju, B.K. Flexible organic phototransistors based on a combination of printing methods. *Org. Electron.* **2014**, *15*, 2677–2684. [CrossRef]
15. Kim, Y.H.; Han, J.I.; Han, M.K.; Anthony, J.E.; Park, J.; Park, S.K. Highly light-responsive ink-jet printed 6,13-bis(triisopropylsilylethynyl) pentacene phototransistors with suspended top-contact structure. *Org. Electron.* **2010**, *11*, 1529–1533. [CrossRef]
16. Yuan, Y.; Huang, J. Ultrahigh Gain, Low Noise, Ultraviolet Photodetectors with Highly Aligned Organic Crystals. *Adv. Opt. Mater.* **2016**, *4*, 264–270. [CrossRef]
17. Liu, J.; Jiang, L.; Shi, J.; Li, C.; Shi, Y.; Tan, J.; Li, H.; Jiang, H.; Hu, Y.; Liu, X.; et al. Relieving the Photosensitivity of Organic Field-Effect Transistors. *Adv. Mater.* **2020**, *32*, 1–8. [CrossRef]
18. Feng, L.; Jiang, C.; Ma, H.; Guo, X.; Nathan, A. All ink-jet printed low-voltage organic field-effect transistors on flexible substrate. *Org. Electron.* **2016**, *38*, 186–192. [CrossRef]
19. Jiang, C.; Cheng, X.; Tsangarides, C.P.; Su, Y.; Ma, H.; Nathan, A. Ultralow-Power All-Inkjet-Printed Organic Thin-Film Transistors for Wearables. In Proceedings of the 2020 IEEE Electron Devices Technology and Manufacturing Conference, Penang, Malaysia, 6–21 April 2020; pp. 1–4, ISBN 9781728125398.
20. Jiang, C.; Ma, H.; Nathan, A. Stability Analysis of All-Inkjet-Printed Organic Thin-Film Transistors. *MRS Adv.* **2017**, *357*, 1–8. [CrossRef]
21. Jiang, C.; Ma, H.; Hasko, D.G.; Guo, X.; Nathan, A. A Lewis-Acid Monopolar Gate Dielectric for All-Inkjet-Printed Highly Bias-Stress Stable Organic Transistors. *Adv. Electron. Mater.* **2017**, *3*, 1700029. [CrossRef]
22. Feng, L.; Tang, W.; Zhao, J.; Yang, R.; Hu, W.; Li, Q.; Wang, R.; Guo, X. Unencapsulated Air-stable Organic Field Effect Transistor by All Solution Processes for Low Power Vapor Sensing. *Sci. Rep.* **2016**, *6*, 20671. [CrossRef] [PubMed]
23. Sze, S.M. *Physics of Semiconductor Devices*, 2nd ed.; Wiley: Hoboken, NJ, USA, 1981.
24. Wasapinyokul, K.; Milne, W.I.; Chu, D.P. Origin of the threshold voltage shift of organic thin-film transistors under light illumination. *J. Appl. Phys.* **2011**, *109*, 084510. [CrossRef]
25. Jeon, S.; Ahn, S.E.; Song, I.; Kim, C.J.; Chung, U.I.; Lee, E.; Yoo, I.; Nathan, A.; Lee, S.; Robertson, J.; et al. Gated three-terminal device architecture to eliminate persistent photoconductivity in oxide semiconductor photosensor arrays. *Nat. Mater.* **2012**, *11*, 301–305. [CrossRef]

26. Kazim, S.; Ramos, F.J.; Gao, P.; Nazeeruddin, M.K.; Grätzel, M.; Ahmad, S. A dopant free linear acene derivative as a hole transport material for perovskite pigmented solar cells. *Energy Environ. Sci.* **2015**, *8*, 1816–1823. [CrossRef]
27. Usta, H.; Kim, D.; Ozdemir, R.; Zorlu, Y.; Kim, S.; Ruiz Delgado, M.C.; Harbuzaru, A.; Kim, S.; Demirel, G.; Hong, J.; et al. High Electron Mobility in [1]Benzothieno[3,2- b][1]benzothiophene-Based Field-Effect Transistors: Toward n-Type BTBTs. *Chem. Mater.* **2019**, *31*, 5254–5263. [CrossRef]
28. Theodosiou, A.; Kalli, K. Recent trends and advances of fibre Bragg grating sensors in CYTOP polymer optical fibres. *Opt. Fiber Technol.* **2020**, *54*, 102079. [CrossRef]